

# Electroreduction Processes of Composite Anodic Passive Layers on Lead in Sulphuric Acid Solution at Temperatures in the 0-50 °C Range

Francisco E. Varela, Liliana M. Gassa and Jorge R. Vilche

*Instituto de Investigaciones Fisicoquímicas Teóricas y Aplicadas (INIFTA),  
Facultad de Ciencias Exactas, Universidad Nacional de La Plata,  
Sucursal 4, C.C. 16, (1900) La Plata, Argentina*

Received: July 13, 1992

O processo de eletroredução de camadas do composto de sulfato de Pb(II)-óxido, formadas anodicamente em eletrodos de chumbo de alta pureza foi investigado em solução de ácido sulfúrico no intervalo de 0-50 °C. O estudo cinético de transiente-potenciostático foi complementado com dados obtidos usando uma combinação de técnicas de voltametria, ajustando adequadamente a formação da camada anódica e as condições de eletroredução.

Os processos de eletroredução das superfícies contendo espécies de Pb(II) podem ser interpretados em função de mecanismos de nucleação de complexos e de crescimento, onde as energias de ativação dos estágios de reação correspondentes foram calculados a partir da dependência da temperatura dos parâmetros cinéticos obtidos pelos procedimentos não-lineares de ajustes.

The electroreduction processes of composite lead (II) sulphate-oxide layers anodically formed on high purity lead electrodes have been investigated in sulphuric acid solution in the temperature range 0-50 °C. The transient potentiostatic kinetic study was complemented with data obtained using combined voltammetry techniques by properly adjusting both the anodic layer formation and the electroreduction conditions. The electroreduction processes of the Pb(II)-containing surface species can be interpreted in terms of complex nucleation and growth mechanisms, where the corresponding activation energies of reaction stages were calculated from the temperature dependence of the kinetic parameters obtained by non-linear fit procedures.

**Key words:** *lead/sulphuric acid electrode; composite; lead sulphate-oxide; temperature effects.*

## Introduction

The lead-acid battery is one of the most successful electrochemical system for energy storage, particularly in automotive application. In contrast, with the great number of investigation concerning the electrochemical behavior of Pb in H<sub>2</sub>SO<sub>4</sub> solutions, there are relatively few studies on the influence of the temperature on the electrode reaction kinetics of the system<sup>1</sup>. The effect of elevated and variable temperature on the performance of lead-acid batteries has been analyzed<sup>2</sup> under simulated service conditions. In this case, it was found that failures at low-temperature operation can be attributed to both the irreversible sulphation of a few positive plates and morphological changes in the positive active material, whereas at high temperatures the positive-plate composition is more uniform and failure is associated with negative-plate deterioration and/or corrosion of positive grids. A spectrum of charge input rates at low temperatures depending on rate and temperature conditions of the previous discharge has been recently determined<sup>3</sup>, being this

result probably related to PbSO<sub>4</sub> crystal size and non-equilibrium electrolyte concentration in the pores of the electrodes. Likewise, the influence of additives like lignosulphonate expander materials, has been analyzed attempting to improve the performance of the lead-acid battery at low-temperature<sup>4</sup>, taking also into account that one mode of expander action is to change the mechanism of current limitation in the passivation process.

On the other hand, the influence of temperature on the potentiostatic current data for the oxidation kinetics of anodic films on Pb in H<sub>2</sub>SO<sub>4</sub> solutions has been also discussed<sup>5,6</sup>, playing indeed an important role the effects on desorption of water, dehydration of ions, and ionic diffusion and equilibria. The variation of the nucleation and growth rate constants with potential, solution composition, and temperature appears to be strongly dependent on the initial sulphate layer formation conditions.

The present paper reports the influence of temperature on the electroreduction process of the anodic layers formed on

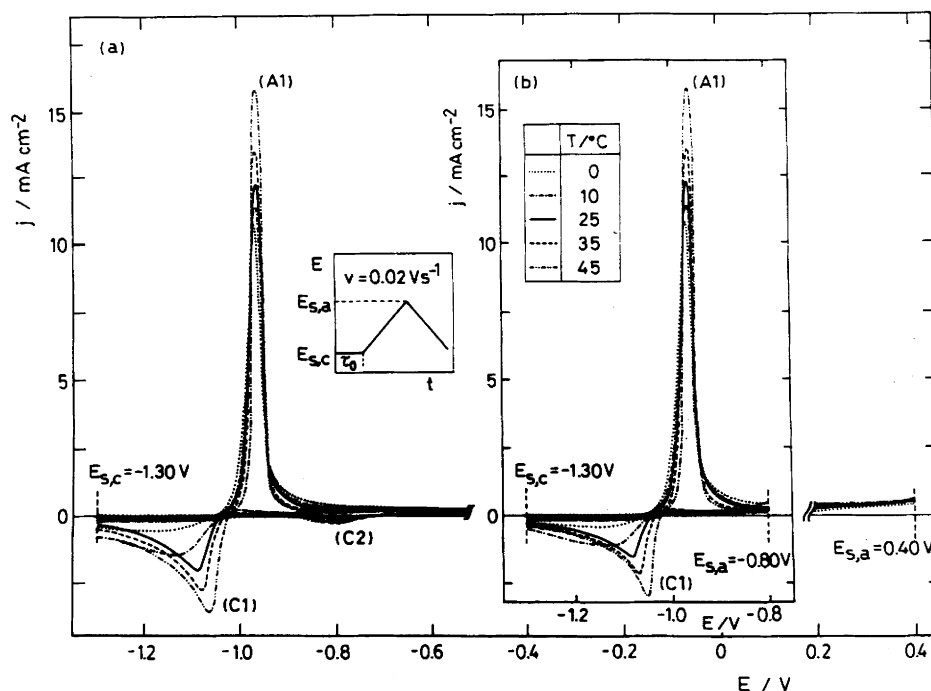


Figure 1. Voltammograms run at  $v = 0.02 \text{ V s}^{-1}$  between  $E_{s,c} = -1.30 \text{ V}$  and  $E_{s,a} = 0.40 \text{ V}$  (a) or  $E_{s,a} = -0.80 \text{ V}$  (b).

lead in  $\text{H}_2\text{SO}_4$  solution in the 0–50 °C temperature range. The study was made employing combined voltammetry and potentiostatic current transient techniques in order to evaluate temperature effects on the nucleation and growth mechanisms, which were satisfactorily used in previous works<sup>7,8</sup> to interpret quantitatively the electroreduction kinetics of  $\text{PbSO}_4$  and  $\text{PbO}$  layers at 25 °C. Besides confirming the model recently elaborated, the present results furnish additional data related to the energies of the involved processes and allow a new insight about the influence of temperature on the performance of the lead-acid battery.

### Experimenta!

The experimental setup was described in previous publications<sup>7,8</sup>. “Specpure” lead discs (Johnson Matthey Chemicals Ltd., 0.30  $\text{cm}^2$  apparent area) embedded in PTFE holders were used as working electrodes in 5 M  $\text{H}_2\text{SO}_4$ , under purified nitrogen gas saturation. The electrolyte solution was prepared from analytical grade (p.a. Merck) reagents and triply-distilled water. Measurements were made at five temperatures between 0° C and 50° C. Lead electrodes were mechanically polished with 600 grade emery papers and thoroughly rinsed in triply-distilled water. Potentials were measured against a  $\text{Hg}/\text{Hg}_2\text{SO}_4$ ,  $\text{K}_2\text{SO}_4$  (sat.) reference electrode (0.680 V in the NHE scale).

Prior to the electrochemical experiments the working electrodes were cathodized during  $\tau_0 = 5$  min at potentials located in the net hydrogen evolution reaction range to achieve a reproducible electroreduced Pb surface. The following potential programs were applied: (i) single (STPS) or repetitive (RTPS) triangular potential sweeps between preset cathodic ( $E_{s,c}$ ) and anodic ( $E_{s,a}$ ) switching potentials at a scan rate ( $v$ ) in the range  $0.002 \text{ V s}^{-1} \leq v \leq 0.200 \text{ V s}^{-1}$ ; and (ii) potential steps, usually two potential steps covering different potential regions, holding the first potential step

( $E_i$ ) for a certain time ( $\tau$ ) to modify the total amount of the surface products in the anodically formed layer, and the second potential step ( $E_f$ ) was set sufficiently negative to electroreduce the anodic layer either partially or completely.

### Results and Discussion

The voltammograms of lead in 5 M  $\text{H}_2\text{SO}_4$  at  $v = 0.02 \text{ V s}^{-1}$  run between  $E_{s,c} = -1.30 \text{ V}$  and  $E_{s,a} = 0.40 \text{ V}$  at different temperatures are shown in Fig. 1a. The voltammetric response shows during the positive going potential sweep a peak A1, attributed to the oxidation of Pb to Pb(II) species. From the thermodynamic standpoint the onset of anodic current can be observed when the applied potential scan reaches a value close to the calculated Pb/PbSO<sub>4</sub> equilibrium potential<sup>9</sup>. The cathodic processes occurring in the potential ranges of peaks C2 and C1 can be associated with

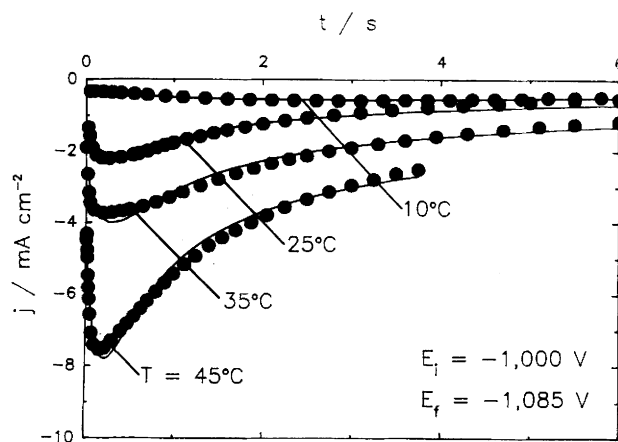


Figure 2. Fitting of current transient data recorded at different temperatures and  $E_f = -1.085 \text{ V}$  after a potential holding at  $E_i = -1.000 \text{ V}$  during  $\tau = 3$  min, according to Eq. 1 (full traces).

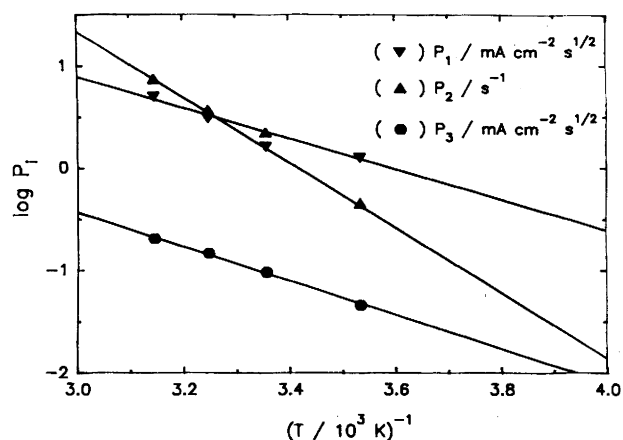


Figure 3. Dependence of  $P_1$ ,  $P_2$ , and  $P_3$  on temperature. Data related to current transients depicted in Fig. 2.

the electroreduction of PbO and PbSO<sub>4</sub> layers, respectively. The location and magnitude of peak C2 depend strongly on  $E_{s,a}$ , ie for  $E_{s,a} \leq -0.40$  V the current contribution of peak C2 is not observed (Fig. 1b). The detailed analysis of these voltammograms at 25° C has been given elsewhere<sup>8</sup>. In the present paper voltammograms are described with the purpose to show the deactivation of both electrooxidation and electroreduction process taking place according to the decrease of temperature. This is clearly observed, for instance, in the remarkable temperature-dependence of the whole voltammetric charge density.

The potentiostatic current transients obtained for the electroreduction of PbO and PbSO<sub>4</sub> layers, varying  $E_i$  and  $E_f$  at convenience, correspond to nucleation and growth processes of new phases, being the new results of measurements performed at temperatures within the 0-50 °C range in accordance with the earlier proposed kinetic models<sup>7,8</sup>. The kinetic study was conducted at temperature up to 50 °C tak-

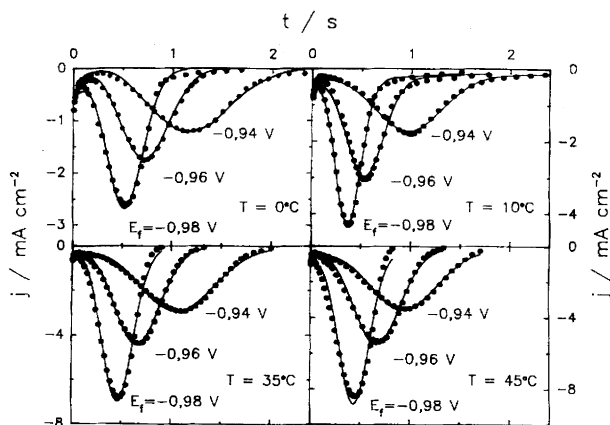


Figure 4. Fitting of current transient data recorded at different temperatures and  $E_f$  in the -0.98 V to -0.94 V potential range after a potential holding at  $E_i = 0.40$  V during  $\tau = 30$  s, according to Eq. 2 (full traces).

ing into account that at about 60° C a degradation in operational life of automotive batteries is usually observed<sup>2</sup>.

The electroreduction kinetics of the PbSO<sub>4</sub> layer can be interpreted through an instantaneous nucleation and 3D growth process under diffusion control by<sup>10</sup>

$$j(t) = P_1 t^{1/2} [1 - \exp(-P_2 t)] + P_3 t^{1/2} \quad (1)$$

where  $P_1 = z F D^{1/2} c \pi^{-1/2}$ ,  $P_2 = N_o \pi K D$ , and  $P_3 = z D_s^{1/2} c_s \pi^{-1/2}$ . The diffusion coefficients  $D$  and  $D_s$ , and the concentrations  $c$  and  $c_s$ , correspond to the involved species in the passive layer solution, respectively,  $K = (8 \pi c M \rho^{-1})^{1/2}$ , and  $N_o$  are the nuclei instantaneously formed. The good agreement between experimental and calculated data, the latter evaluated from Eq. 1, is shown in Fig. 2 for  $E_i = -1.00$  V ( $\tau = 3$  min),  $E_f = -1.085$  V, and different temperatures. The calculated parameters  $P_i$  ( $i=1,2,3$ ) increase with temperature obeying an Arrhenius behavior, according to the linear  $\log P_i$  vs.  $1/T$  relationships depicted in Fig. 3. Accordingly, the value of  $\Delta \ln P_i / \Delta(RT)$  is close to  $-30$  kJ mol<sup>-1</sup> for both  $P_1$  and  $P_3$ , whereas for the case of  $P_2$ , it increases to about twice of that value. The results are in accordance with the physicochemical terms involved in the  $P_i$  parameters.

On the other hand, the cathodic current transients obtained for PbO electroreduction process can be appropriately described by the expression:

$$j(t) = P_4 [1 - \exp(-P_5 t^3)] \exp(-P_6 t^3) + P_7 \exp(-P_7 t) \quad (2)$$

which corresponds mainly to a progressive nucleation and 3D growth under charge transfer control<sup>11</sup>. In Eq. 2 growing nuclei are considered to be right circular cones distributed at random on a planar electrode surface, whereas the second term, which predominates only at very short times, can be related to an instantaneous nucleation and 2D growth under diffusion control<sup>12</sup>. The parameters are given by  $P_4 = z F k_1$ ,  $P_5 = \pi M^2 k_2^2 A/3 \rho^2$ ,  $P_6 = q_{mon} \pi K_h D_h N'_o$ , and  $P_7 = \pi K_h D_h N'_o$ , where  $k_1$  and  $k_2$  denote the rate constants describing crystal growth parallel and perpendicular to the plane surface electrode, respectively,  $A$  is the nucleation

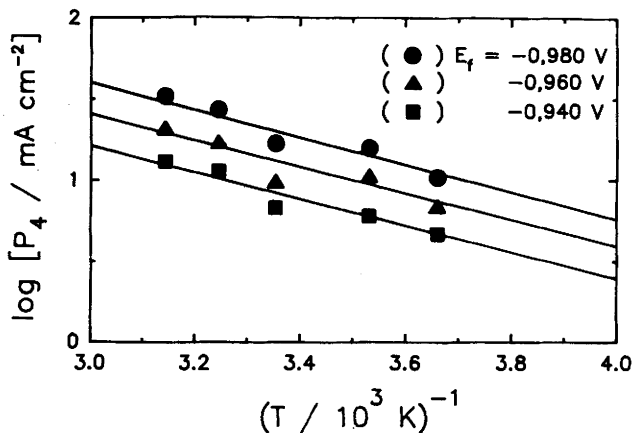


Figure 5. Dependence of  $P_4$  on temperature at different  $E_f$ . Data related to current transients depicted in Fig. 4.

rate constant,  $q_{\text{mon}}$  the monolayer charge density,  $K_h = (8\pi c_h M \rho^{-1})^{1/2}$ , and  $N'$ , the number of active centers. Fig. 4 illustrates the good agreement between experimental and calculated data. It is worth noting that there is an increase of the charge density related to the PbO electroreduction on raising the temperature from 0 to 50 °C, being this effect considerable smaller than that associated with the PbSO<sub>4</sub> electroreduction. At each temperature value, it is possible to calculate an optimal set of fit parameters. The temperature dependence of  $P_4$  is shown in Fig. 5 at different  $E_f$ . It was found that at constant  $E_f$ ,  $P_5$  as well as  $P_6$  and  $P_7$  reveal to be practically independent on temperature. It is interesting to note that the  $\log P_4$  vs.  $1/T$  Arrhenius plot (Fig. 5) approaches a linear relationship for the rate constant for the phase growth parallel to the surface, whereas the corresponding activation energy results lower than that above calculated for the PbSO<sub>4</sub> reduction.

### Conclusions

The kinetic data analysis allows to conclude that the nucleation and growth mechanisms employed recently to interpret the electroreduction of PbO and PbSO<sub>4</sub> at room temperature, can be successfully used in 0 to 50 °C temperature range. The electroreduction of PbSO<sub>4</sub> porous layer involves an instantaneous nucleation and three dimensional growth mechanism under diffusion control, and the electroreduction of the PbO layer, which builds up progressively beneath the initially grown PbSO<sub>4</sub> layer, can be related to a progressive nucleation and 3D growth mechanism under charge transfer control.

### Acknowledgments

This research project was financially supported by the Consejo Nacional de Investigaciones Científicas y Técnicas, the Comisión de Investigaciones Científicas de la Provincia de Buenos Aires, and the Fundación Antorchas. Part of the equipment used in the present work was provided by the DAAD and the von Humboldt-Stiftung.

### References

1. K.R. Bullock and D. Pavlov (Editors), *Advances in Lead-Acid Batteries*, The Electrochemical Society Inc., Pennington, NJ (1984).
2. D.C. Constable, J.R. Gardner, K. Harris, R.J. Hill, D.A.J. Rand and L.B. Zalcman, *J. Electroanal. Chem.* **168**, 395 (1984).
3. T.F. Sharpe and R.S. Conell, *J. Appl. Electrochem.* **17**, 789 (1987).
4. P.J. Mitchell, N.A. Hampson and J. Smith, *J. Appl. Electrochem.* **12**, 13 (1982).
5. M. Fleischmann and H.R. Thirsk, *Trans. Faraday Soc.* **51**, 71 (1955).
6. E.M.L. Valeriotte and L.D. Gallop, *J. Electrochem. Soc.* **124**, 380 (1977).
7. F.E. Varela, L.M. Gassa and J.R. Vilche, *Anais VII Simpósio Brasileiro de Eletroquímica e Eletroanalítica*, Ribeirão Preto, 482-88 (1990).
8. F.E. Varela, L.M. Gassa and J.R. Vilche, *Electrochim. Acta* **37**, 1119 (1992).
9. F. Letowski and G. Pinard-Legry, *Electrochim. Acta*, **26**, 245 (1981).
10. B.R. Scharifker and J. Mostany, *J. Electroanal. Chem.*, **117**, 13 (1984).
11. R.D. Armstrong, M. Fleischmann and H.R. Thirsk, *J. Electroanal. Chem.*, **11**, 208 (1966).
12. R.D. Armstrong and J.A. Harrison, *J. Electrochem. Soc.*, **116**, 328 (1969).